Infrared thermography based fuel film investigations

F. Schulz*, J. Schmidt,
Institute of Fluid Dynamics and Thermodynamics
Otto-von-Guericke University Magdeburg
PO 4120, 39106 Magdeburg, Germany
florian.schulz@ovgu.de and juergen.schmidt@ovgu.de

Abstract

In this paper we present an infrared thermography based method for systematic studies of the temporal and spatially resolved heat fluxes during the whole process of spray impingement to film evaporation. This is mainly possible due to new developments in infrared camera technology. The influence of three test parameters was examined - the injector position, the injection pressure and the wall temperature.

Fuel wall films are an important origin of soot particles in GDI engines. In order to reduce fuel wetting a detailed analysis of wall film forming is necessary. The strong influence of the surface temperature on the droplet-wall interaction and the resulting liquid deposition is known. But the quantitative forecast of wall films caused by dense sprays is usually poor because of the various parameters influencing the occurring heat fluxes which reduce the surface temperature during the injection.

The maximum temperature decrease of the wall is sensitive to all three test parameters. The overall heat inserted into the fuel is almost independent of the distance between injector and wall. Contrary to the first guess that the spray impact takes more energy out of the wall than the following film evaporation it can be shown that underneath the Nukiyama-Temperature the film evaporation needs up to 15 times the heat used during the spray-wall interaction.

Introduction

Modern gasoline engines usually use the principle of direct injection. The fuel is injected at pressures up to 20 MPa into the combustion chamber. If the fuel reaches the piston or cylinder walls prior to its complete evaporation, the spray droplets contact the surface. As a result of the spray-wall interaction the wall film occurs in particular on the piston surface and is the cause of high soot emissions.

The spray-wall interaction is known from diesel engines [1] and the Throttle-body injection [2] and has been extensively tested for this. The boundary conditions, for example, the injection pressure, the combustion chamber temperature, the combustion chamber pressure, the wall geometry or the wall temperature differ substantially from the conditions in the combustion chamber of the gasoline engine. For this reason, the measured values and derived models are not easily transferred to the processes in a gasoline engine. Therefore new tests are necessary which are adapted for the gasoline engine.

The literature offers extensive studies on the interaction of single droplets with walls [3] and there impact regimes were found. However, in DI-sprays strong interactions and spatial and temporal overlap of physical phenomena appear. That is why the transfer of the results is possible only to a limited extent. Investigations by Richter [4] showed in relation to the secondary droplet formation during the impact of drops in the micro-and millimeter-range significant differences. Statements relevant to the wall film behavior at different operating points are attainable only through the study of real sprays. These primarily include optical measuring methods for visualization of the liquid film and the fuel vapor fraction [5]. Occasionally transient wall temperature measurements using thin-film and other sensors with short time response are done. Temperature measurements which are co-relatable with the heat flow are suitable for quantitative characterization of fuel films [6] and at the same time allow the validation of the appropriate, mostly CFD-based, simulations [7].

With the help of infrared thermography, the unsteady wall temperature gradients can be determined without contact and almost instantaneously. Especially the high-resolution temperature information across the entire film allows new findings in comparison to similar point wise method. Because of its speed and robustness the measuring method allows systematic measurements over a wide range of parameters. These statements include the effect of spray shape, orientation, operating pressure, injection quantity and the regime as well as distance from the wall and the initial wall temperature. The results can be used to adjust and to develop simulation models, and thus serve the combustion process development.

* Corresponding author: florian.schulz@ovgu.de

Wall films – basic effects

The parameters effecting the wall film forming and evaporation are illustrated in figure 1. One of the most important boundary conditions that affect the resulting wall film, is the injector. Due to its design a characteristic spray shape and specific droplet parameters are generated. Depending on the droplet velocity and diameter and the fuel properties the liquid deposition will be characteristic. Beside the spray-wall interaction and the liquid deposition the film propagation can take place. It is induced by droplet momentum and air flow of the entrained air. This is a dominating effect for the wall film size, shape and distribution.

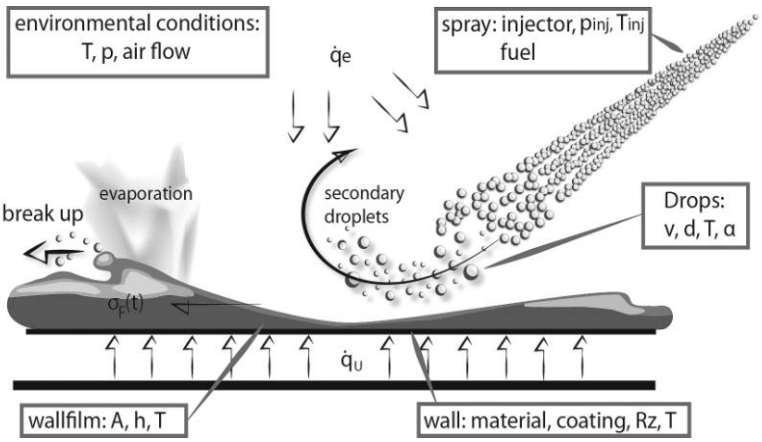

Figure 1 Spray-wall interaction: parameters and effects

The wall features represent another major boundary condition to be mentioned at this point. The wall influences the occurring heat fluxes and therefore the spray-wall interaction, the film propagation, and the film evaporation. In case of the soot particles exhausted by GDI engines of course liquid deposition should be avoided but it would be also sufficient if an appearing film evaporates fast enough before ignition starts. And that depends on the distribution of the wetted area and the heat inserted through the wall. With the method described below we are able to find space and time resolved heat fluxes and thus can determine the wall temperatures.

Experimental Methods

The focus of this study is basic research on the infrared thermographic investigations of the spray-wall interaction and liquid films. Therefore, the injection process of the real homogeneous charged Otto engine is simplified by the spray application at different boundary conditions on a heated plate. Figure 2 illustrates the position of the IR8800 infrared camera underneath the sheet.

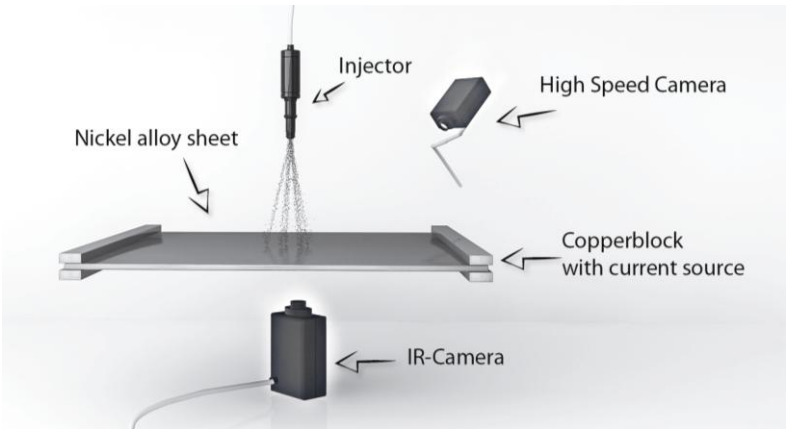

Figure 2 Schematic experimental setup

The electrically heated plate has a size of 100 x 150 mm^2, consists of a nickel alloy and has a special coating with the thickness of 40 µm at the back to achieve a high emissivity. With the aid of the electrical power supply the wall temperature can be controlled and is set to a constant value before spray impact. The detailed description of the pressure generation and calibration of the measuring system is found in the X. Proceedings Engine combustion [8]. The used injector is a common high-pressure six hole nozzle controlled by a magnetic system.

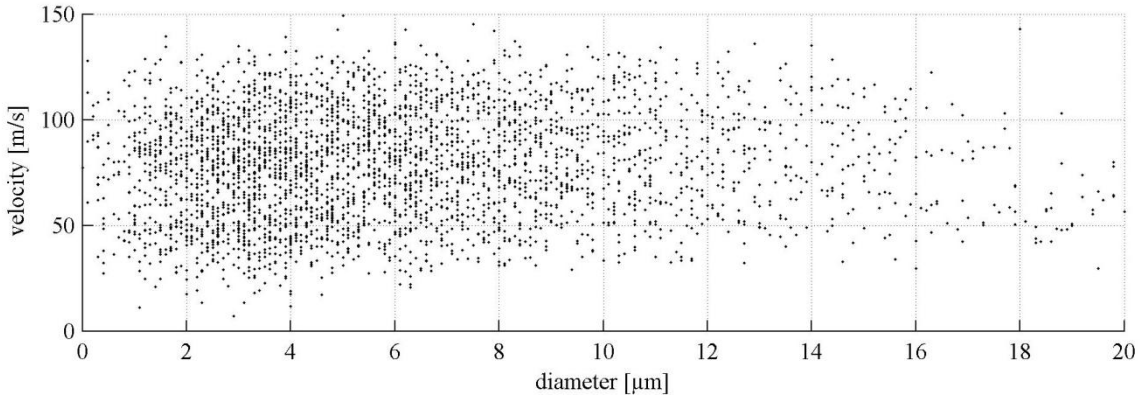

Figure 3 PDA results: droplet diameter and velocity distribution of the spray, a=35mm, p_{inj}=15MPa

For this paper boundary conditions with an injection pressure of p_{inj}=15MPa, an injected gasoline mass m_{fuel}=21,7mg, distance nozzle-wall a=35mm and wall temperature T=80°C under environmental conditions are chosen as the point of comparison. For this set up the spray characteristics determined with PDA measurements are illustrated in Figure 3. The injector creates a dense gasoline spray with an average diameter of d_{10} = 4.5µm and an average velocity of 75m/s. Beside PDA measurements back-light images of a spray are commonly used to verify spray models. Because this technique is a comparatively easy way to get information about the distribution of the whole liquid spray, in opposite to the PDA which is a punctually method. Using the presented technique of infrared measurements a series of images like figure 4 are obtained. These recordings give information about the whole spray and additionally about the wall film. Therefore it provides a way to compare injectors, control spray targeting and to verify simulations. The level of detail should be emphasized. Even the finger-like jets generated by the dynamic liquid film are visible.

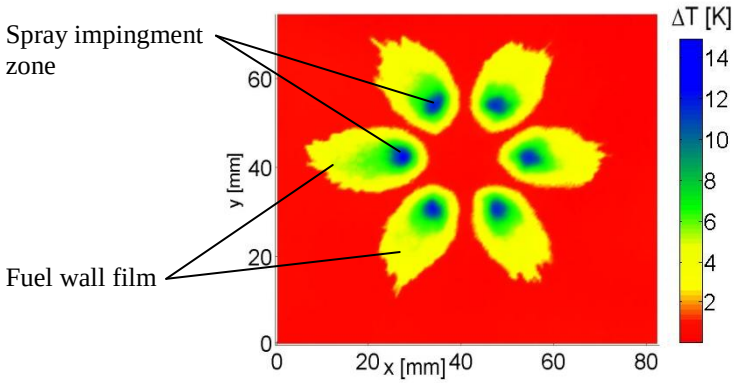

Figure 4 Field of temperature differences of the fuel wall film caused by a six hole nozzle, p_{inj}=15MPa, a=35mm, T=80°C

To use this setup for heat flux evaluations it must be verified that the behavior of the surface temperatures on the sheet are comparable to those of a half space body, as which a piston can be considered. Therefore the simulation results for a simplified spray impact case are shown in figure 5. Here you see the influence of a negative heat flux on the surface temperatures of a 0.1mm, 0.2mm and 5mm nickel alloy sheet. The used constant heat flux of -3.1 MW/m^2 is an average value for the considered spray-wall-system with an initial wall temperature of 80°C and injection duration of 1.5ms at p_{inj}=15MPa.

The diagram shows that the extracted heat generates an enormous temperature decrease of 17K at the surface. From the beginning to the end of the injection, the temperature is almost independent of the sheet thickness. This means that the experimental method can be used without limitations for the investigation of the spray wall interaction. The same statement applies to the process of wetting and propagation of the wall film, because this is also completed within a few milliseconds. But for the study of film evaporation, the significant temperature differences between the sheets after about 12ms, have to be considered. For the film evaporation the surface temperatures in the experiment are lower than they would be on the piston. In the diagram the temperature which appears after the relaxation is only dependent on the inner energy of the sheet and therefore indirect proportional to the thickness. With the help of the simulation the temperature profile that would occur for a half space can be determined. So the half space temperatures can be included in further analysis. This proceeding can be done

quite well within one heat transfer regime namely the film evaporation regime, the nucleate boiling regime and the film boiling regime because in these regions the physical phenomena are stable. Here, a little difference in the surface temperature generates only slight changes in the heat flux. But if the surface temperature exceeds the limits of regimes, then the influences of individual effects can change. In the transition boiling regime slight temperature changes can generate major differences of the heat flux. The evaluation needs to be done careful for this regime.

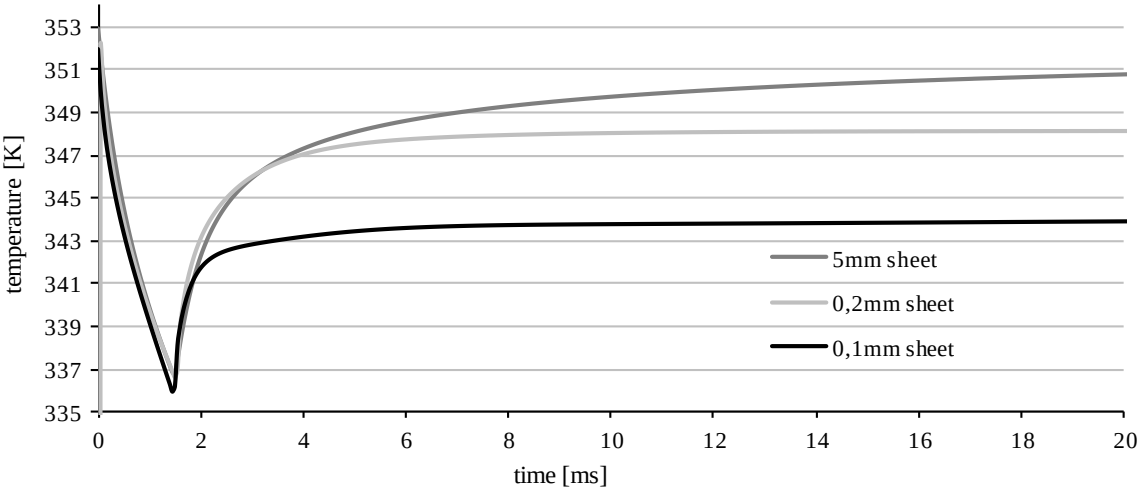

Figure 5 Simulated sheet temperatures on the surface for a 1.5ms lasting heat flux of 3.1 MW/m^2 for nickel alloy sheets of a 0.1mm, 0.2mm and 5mm considering only heat conduction

To give an idea of what is happening within and underneath the sheet, figure 6 is plotted below. Here the same heat flux like in figure 5 is influencing the sheet temperature. For the simulation the sheet properties are the same as in the real experiment. The heat conduction passes 0.1mm of the nickel alloy and afterwards 0.04mm of black coating. The top and back temperatures converge at about 16ms. That means the measured temperatures with the infrared camera of the coated back do not match with the top surface temperatures. Therefore an inverse calculation is necessary to find the top surface temperatures out of the measured temperature field sequences. A simplified approach is described below. From figure 5 and figure 6 improvements of the experimental setup can already be deduced. Considering film evaporation a thicker sheet would lead to top surface temperatures with a closer relation to a half space body. Beyond this the conductivity of the coating is small compared to the metal. A reduced thickness or a different material could reduce relaxation time.

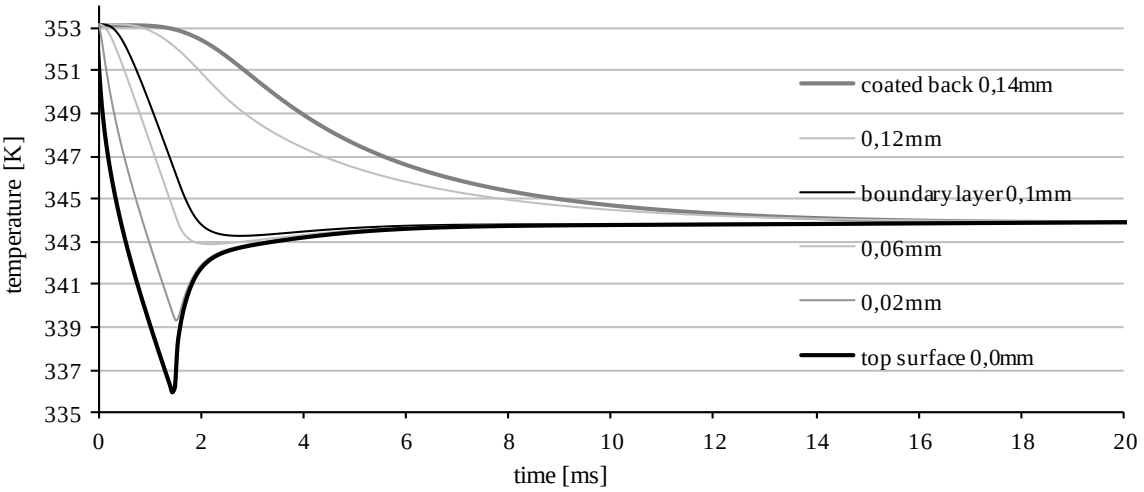

Figure 6 Simulated temperatures within a 0.1mm nickel alloy sheet with a 40µm coating on the back due to a constant heat flux of 3.1 MW/m^2 with a duration of 1.5ms

This article focuses on the heat fluxes and temperatures. For this reason, two further possibilities of the method are mentioned only briefly. First it is feasible to find the quantitative sizes of the wall film areas, but also their qualitative shapes as figure 7 illustrates. So a further way of comparison is provided. Another achievement of the infrared method is the information of the heat flux distribution over time. Figure 8 shows fields of the heat fluxes of one spray jet over time. Because of the spray pulse, a large portion of the fuel is flowing into the outlet

region of the spray impact and remains there as agglomerated wall film. Because of the greater film thickness in this area the evaporation time is enlarged.

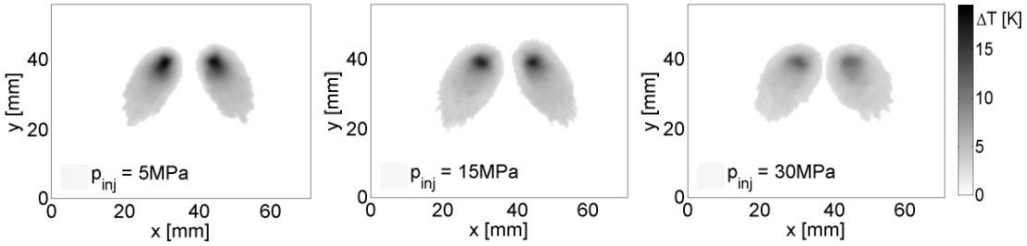

Figure 7 Wall film shapes, a = 25mm, T_{sheet} = 80°C

At the beginning of the injection (t1) heat is removed only at the impact zone. Then the film propagates (t2). In the third picture (t3), the injection is now complete and the fuel evaporates. Finally, at the time t4, the wall film is already evaporated at the spray impact zone. Heat is transferred only in the outlet region because there still is liquid fuel. This area of the wall film forms the basis for the particle formation. Since liquid fuel which is not evaporated before ignition starts, finds ideal conditions for the conversion into carbon black.

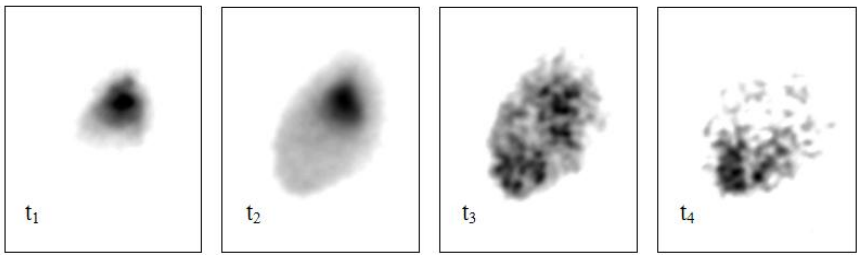

Figure 8 Qualitative illustration of the heat flux over time, a = 35mm, T_{sheet} = 80°C, p_{inj} = 15MPa

Results and Discussion

The following discussion distinguishes between the spray impact zone and the wall film zone. For the spray impingment zone the injection event can roughly be divided into three phases. First, the spray impacts for the duration of the injection with a high heat flux. Then follows a phase of movement of the shear stress-driven liquid. The movement improves the heat transfer between wall and fluid. The third stage is that the residual liquid evaporates while the heat flux is comparatively low. Contrary to the spray impact zone the process of droplet impingment is missing in the wall film zone. The first phase which starts during the injection is the liquid propagation which is mainly driven by the droplet impulse. This phase is characterized by a high velocity and it keeps on going even after injection has finished because of the entrained air and the impulse of the film. In the second phase the movement in the inner region has already stopped and in the outlet region the liquid movement slows down and the film reaches its maximum size. The third phase contains the residual liquid evaporation and Marangoni convection. The time durations for the phases were taken out of top view high-speed recordings of the spray-wall interaction.

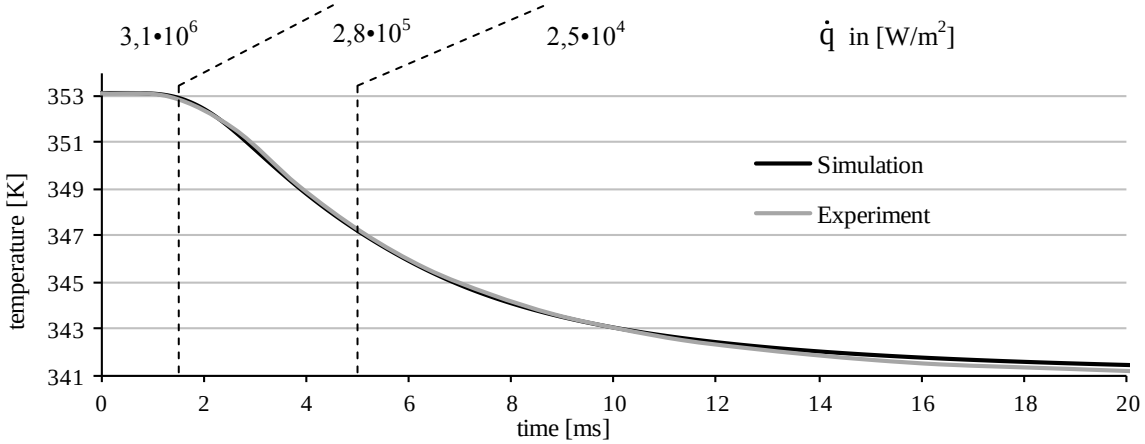

Figure 9 Spray impact zone: Comparison between the average measured temperature and the simulation

As mentioned above the infrared measured temperature fields need an inverse calculation in order to find the real surface temperatures and heat fluxes. The diagram of Figure 9 shows an example case of a simplified iterative method to determine the heat fluxes at the spray-wall boundary. Therefore a conduction simulation with rational heat fluxes for the described three phases within the spray impact zone was carried out. Subsequently the simulated temperature progress was compared to the measured data and with an adoption of the three heat fluxes a new simulation was started. After the third run the temperature curves of the simulation and the measurement were adjusted. For the conditions in figure 9 a distance injector-wall of 35mm, a pressure of 15MPa, an injection time of 1.5ms and a sheet temperature of 80°C were chosen. The resulting heat fluxes are $3.1 \cdot 10^6$ W/m^2 during the injection process, $2.8 \cdot 10^5$ W/m^2 when the liquid moves until 5ms and $2.5 \cdot 10^4$ W/m^2 while evaporation. The behavior of the calculated heat fluxes is reasonable. The high heat flux at the beginning causes a temperature decrease up to 18K at the top surface. Until 5 ms the surface temperature rises by 5K due to heat conduction from the sheet and a reduced heat flux at the liquid-solid boundary. After 20ms the backside temperature almost matches the top surface temperature of 341K with a difference of 1K.

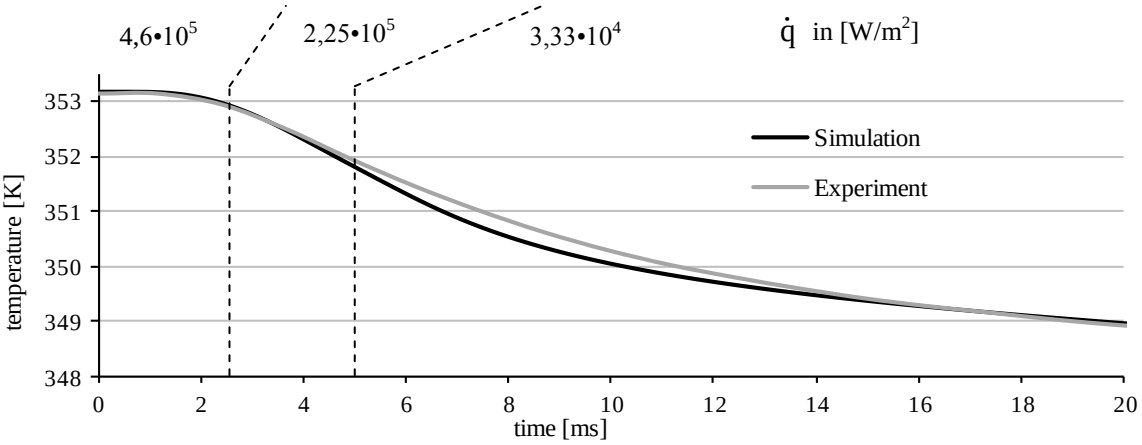

Figure 10 Wall film area: comparison between the average measured temperature and the simulation

Under the same conditions but considering the wall film zone, figure 10 provides the temperature information. It is complicated to catch one temperature curve for the whole wall film area. Therefore the average temperature was used. During the phase of liquid propagation within the first 2.5ms the heat flux reaches $4.6 \cdot 10^5$ W/m^2. The slow moving phase is characterized by almost $2.3 \cdot 10^5$ W/m^2. The residual liquid evaporation begins at 5ms and takes a heat flux of about $3.3 \cdot 10^4$ W/m^2 out of the wall. The values of the first two phases are comparatively large considering that there is only the convection of a moving liquid. The heat flux of the third phase does match the value of the impingment zone. It is explainable that the value for the wall film evaporation phase is lower in the spray impact zone because of the lower surface temperature and the thinner film. After 20ms the average top surface temperature in the wall film zone is 348.5K, that means 7.5K above the average temperature of the spray impact zone. At this time the evaporation is not finished. For predictions of evaporation time and fuel mass left on the piston, the top surface temperature is a key parameter because it influences the evaporation speed.

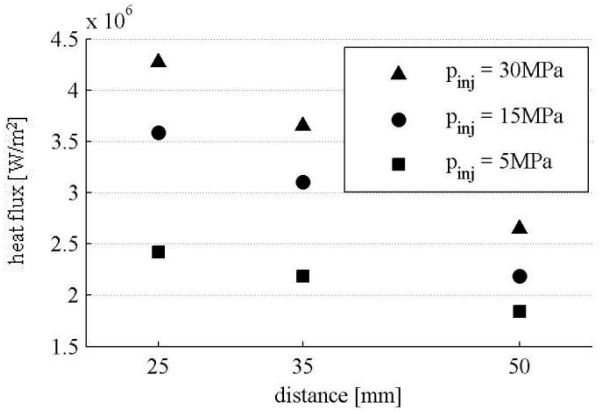

Figure 11 Heat flux at the spray impact zone, T_{sheet} = 80°C

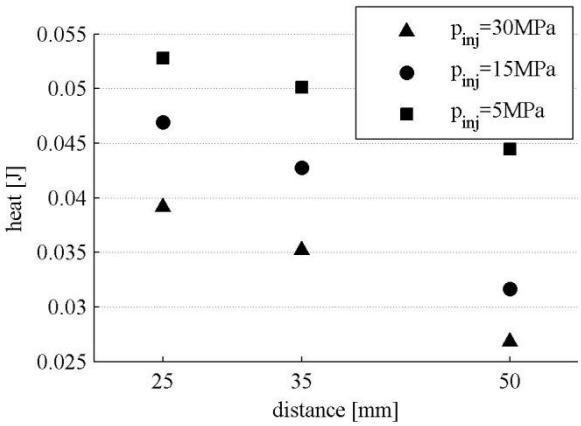

Figure 12 Heat removal at the spray impact

Figure 11 summarizes the calculated heat fluxes for the spray-wall interactions with injector-wall distances of 25, 35 and 50mm and injection pressures of 5, 15 and 30MPa for a sheet temperature of 80°C. The injected fuel mass stays the same through adjustment of the injection duration t_{30}=1.06ms, t_{15}=1.5ms and t_5=2.5ms. As expected the greater the pressure and the lower the distance the heat flux increases. But with increasing distance the influence of the pressure decreases. Also interesting is the heat removal out of the solid surface during the injection. Figure 12 reveals that it is not the 30MPa causing the highest heat extract but the 5MPa injection pressure. That is due to the longer injection time. The heat removal is found by integrating the heat flux over the duration time and the impact area. So with smaller injection pressures the same injected mass leads to a higher amount of extracted heat and therefore to a lower top surface temperature. This fact might be important for later film evaporation. In the calculation also the enlarging impact areas with increasing distance and rising pressure are included. But these have little effect.

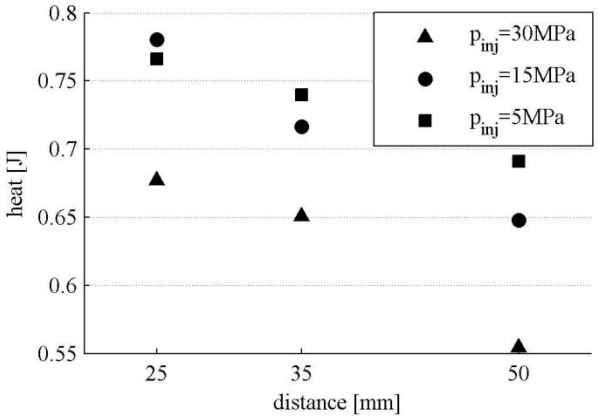

Figure 13 Heat removal at the wall film area

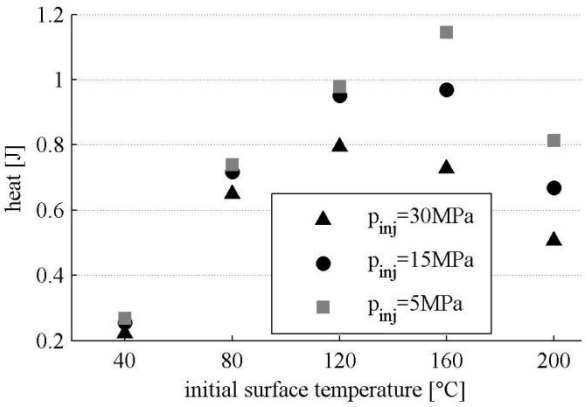

Figure 14 Heat removal at the wall film area, a=35mm

Considering the wall film area a more complex situation is given because the extracted heat depends on the included period of time. For figure 13 and 14 the first 40ms after injection are taken into account. The heat removal at the wall film area is directly related to the deposited fuel mass. This heat for a wall temperature of 80°C is plotted in figure 13. An increasing distance decreases the heat because of the limited penetration. Less fuel reaches the wall. For higher injection pressures usually the overall heat decreases. But the 15MPa injection pressure overtakes the 5MPa at 25mm. That means that the influence of physical effects change for small injector-wall distances within the convective film evaporation regime. Another important fact results from the comparison of figure 12 and 13. The heat removed by the film is one dimension above the heat extraction caused by the spray impact. Therefore the heat inserted into the film through the wall is very important for the fuel film evaporation.

Figure 14 finally shows the relationship between the extracted heat and the initial wall temperature with a distance injector-wall of 35mm. Over the temperature axis the classical Nukiyama distribution shadows in the results. The changing influence of the injection pressure is important to mention. With low sheet temperatures the influence is rare and with 160°C wall temperature the importance is maximized. And the influence of the injection pressure seems to decrease beyond 160°C. The maximum of the extracted heat does not only depend on the initial surface temperature but also on the injection pressure. For rising injection pressures the surface temperature where the peak of the extracted heat occurs, is decreasing.

With higher wall temperatures where most of the evaporation is finished after 40ms a relationship between the heat removal and the deposited fuel mass is feasible. The deposited fuel mass can be calculated with

$$M_f = \frac{Q_w}{c_p \Delta T_{wb} + h_{fg}} . \quad (1)$$

Since the overall mass injected is known with a value of 21.7mg, the mass of one spray jet is 3.6mg. The required heat for evaporation can be estimated with 2J. Comparing this value with the heat in figure 12 less than two percent of the fuel could be vaporized with the energy taken out of the wall. But looking at the wall film values of figure 13 up to a third of the injected fuel is vaporized within the wall film zone.

Summary

One main result of this paper is the verification of the presented infrared thermography bases method. It could be proofed that it is possible to reproduce conditions close to a DI-engine. The high speed infrared technology provides new opportunities to study the wall-film phenomena. It also provides a way to compare injectors, control spray targeting and to verify simulations. The analysis of the heat conduction in the sheet was leading to possible improvements of the experimental setup. An increased sheet thickness could simplify the interpretation of the film evaporation process. Also an adapted coating with a lower heat resistance could increase the temperature response.

For heat flux determination an iterative method was use. The implementation of an automated inverse algorithm is just taking place and will improve the results. The basic phenomena could be described and a comparison of the spray impingment and the wall-film evaporation was presented. The deposited fuel mass is dependent on the injector-wall distances, on the injection pressures and on the initial wall temperature. The deposited mass can be up to a third of the injected fuel mass. Also interesting is the behavior above wall-temperatures of 200°C, here experiments need to be carried out.

The measured results will be verified by Laser-Induced-Fluorescence wall-film experiments and measurements with enlarged boundary conditions within a pressure chamber are in planning.

Acknowledgements

The support with expertise of the Department of Gasoline Systems (Robert Bosch GmbH) and the financial support of the German Research Foundation (DFG-Graduiertenkolleg 1554) are gratefully acknowledged.

References

[1] Stanton D, Rutland C: Modeling fuel film formation and wall interaction in diesel engines. SAE Technical Paper 960628, 1996

[2] Samenfink W, Elsäßer A, Dullenkopf K, Wittig S: Droplet interaction with shear-driven liquid films: analysis of deposition and secondary droplet characteristics. International Journal of Heat and Fluid Flow 20, S. 462–469, 1999

[3] Moreira A L N, Moita A S, Panão M R: Advances and challenges in explaining fuel spray impingement: how much of single droplet impact research is useful? Progress in Energy and Combustion Science 36, S. 554-580, 2010

[4] Richter B: Charakterisierung der Tropfen-Wand-Interaktion im Parameterbereich von Ottomotoren mit Direkteinspritzung. Forschungsberichte aus dem Institut für Thermische Strömungsmaschinen, Band 31, Logos-Verlag, 2007

[5] Kiyotaka S, Tadashi T, Jian G, Yuhei M, Keiya N, Masahisa Y: Analysis of evaporation process on non-axisymmetric wall-impinging spray by means of laser absorption scattering technique. Transactions of the Japan Society of Mechanical Engineers, Part B, Volume 74, Number 8, S. 1853-1859, 2008

[6] Montorsi L, Magnusson A, Andersson S, Jedrezejowski S: Numerical and experimental analysis of the wall film thickness for diesel fuel sprays impinging on a temperature-controlled wall. Diesel Fuel Injection and Sprays, SAE- Spec. Publ, S. 119-130, 2007

[7] Kuhnke D: Spray/Wall-Interaction Modelling by Dimensionless Data Analysis, PhD Thesis, Darmstadt University of Technology, Darmstadt, 2004

[8] Kufferath A, Samenfink W, Hammer J, Schulz F, Könnig M, Schmidt J: Charakterisierung des Wandfilms relevanter Betriebsbedingungen für einen direkteinspritzenden Ottomotor als Grundlage zur Schadstoffminimierung. Motorische Verbrennung (X. Tagung) S. 423-436, ESYTEC Verlag, Erlangen, 2011